Thermal and compositional defects in chemical spray pyrolysed indium selenide (In_2Se_3) thin films: Effects on film properties

COSMAS M. MUIVA[a,c], STEPHEN T. SATHIARAJ[a,c], JULIUS M. MWABORA[b,c]
[a]*Department of Physics, University of Botswana, P/Bag UB-0022, Gaborone, Botswana*
[b]*Department of Physics, University of Nairobi, P.O. Box 30197-00100, Nairobi, Kenya*
[c]*African Materials Science and Engineering Network (AMSEN), a Carnegie IAS-RISE Network*

Polycrystalline In_2Se_3 semiconducting thin films were synthesized by chemical spray pyrolysis and their properties investigated. Strong dependence of structural and opto-electronic properties on film composition was observed. Absorption coefficient (α) at normal incidence was determined and an optimised direct optical band gap (E_g) of 1.92 eV was obtained at a substrate temperature (T_{sub}) of 673 K. Whereas low T_{sub} favoured incorporation of impurities in the films, elevated T_{sub} had the effects of introducing textural and structural defects with modifications in the film properties. The crystallinity of the films increased with switch from chalcogen rich to chalcogen deficient films.

(Received April 18,2011; accepted October 20, 2011)

Keywords: In_2Se_3, Spray pyrolysis, Chalcopyrite buffers, Opto-electronic properties, Energy gap

1. Introduction

Chalcogenides glasses belonging to S, Se and Te in form of sulfides, selenides and tellurides, respectively, are attractive materials for applications such as photo-conducting cells, photovoltaic cells, and other opto-electronic devices [1-3]. Many binary chalcogenides including, CdS, SnSe, AsSe, MoSe, BiSe, La_2Se_3, BiS_2, In_2S_3, SbSe and In_2Se_3 have received attention [3,4]. Chalcopyrite based photovoltaic devices are usually fabricated by forming a p-n heterojunctions of n-type CdS and p-type chalcopyrite thin films. In this type of structure, CdS layer is referred to as a buffer and serves the purpose of not only forming a p-n junction with p-type chalcopyrite absorber, but also as an excellent transparent window for light to go through. Indium selenide shows very significant properties for photovoltaic and photochemical application because of an absorption coefficient arising from an energy gap in the range of solar energy conversion [5]. Moreover, InSe has a reported low density of dangling bonds on the layered surfaces which makes it a potential candidate for heterojunction devices with the advantage of minimal density of interface states [6]. With environmental compatibility of CdS raising concern leading to wide spread restrictions on Cd containing merchandise, alternatives such as In_2Se_3 have been put on the front line towards industrial perfection. Recently, Lee *et al*. (2005) [7] reported a rewritable phase change memory device based on γ-In_2Se_3. In_2Se_3 also shows potential for applications in photochemical devices [8]

In_2Se_3 has been prepared by methods such as evaporation [9], spray pyrolysis [10], laser ablation [11], chemical bath deposition [12], electro-deposition [8], sputtering [13], metal organic chemical vapour deposition [14] and mechanical alloying [15]. Vacuum evaporation, laser and sputtering technologies provide high purity products with ease of smoothness control and good film adhesion. However several draw-backs are associated with these methods including multistep, sophistication, low yield and high vacuum cycles hence raising expenses. It is also difficult to control composition and adopt for large area. Chemical methods are cheaper, throughput, offers easy adoption for large scale and easy control of product composition. However, generally, the end products of chemical technologies are less smooth and prone to impurities. For photovoltaic applications, film roughness is advantageous in scattering and trapping light in the absorber layer [16] therefore this roughness can play to an advantage. One of the current issues in photovoltaic power harvesting is cost and any technique that addresses this aspect is quite attractive. In this study, chemical spray pyrolysis (CSP) path is selected as a fabrication technique because of its cheapness, large scale possibilities and versatility in fixing composition by varying concentration of the starting precursor components [17].

A major drawback in obtaining quality films through the CSP is introduction of impurities, in form of by-products from the partial decomposition of the precursor or from plume-ambient interaction. A few reports on In_2Se_3 by spray pyrolysis exist [9], but little has been achieved in terms of desirable properties such as glasslike In_2Se_3 films owing to these impurities. Moreover, the range of optimum optical band gap (E_g) reported in literature for this material is wide. Pathan *et al*., 2005 [12] has reported a band gap of 2.5 eV from films prepared by chemical bath deposition (CBD), Asabe *et al*., 2008 [18] realized a band gap of 2.35 eV through chemical bath

deposition (CBD) while a band gap of 2.09 eV was reported by Bindu *et al*., 2002 [19], by vacuum evaporation and annealing, 2.15 eV by Clavijo *et al*., 2009 [20] by vacuum evapouration and 1.7 eV in spray pyrolysed films by Bouzouita *et al.,* 2002 [10].

In the preliminaries of this study, the effects of thermal and compositional defects were assessed and it was observed that low substrate temperatures (T_{sub}) increased impurities in the films. On the other hand high T_{sub} reduced impurities but introduced textural and structural defects in the film. Consequently, deposition conditions were tailored to deposit In_2Se_3 thin films with different Se/In ratios and at different T_{sub}. The various structural, optical and electrical parameters are reported and discussed on the basis of effects of compositional, textural and structural changes.

2. Experimental details

In_2Se_3 thin films were prepared by homemade spray pyrolysis equipment from a precursor solution containing Indium (III) chloride ($InCl_3$) and Selenourea ($SeC(NH2)_2$) using nitrogen as a vector gas. The details of the setup are described elsewhere [21]. Initially, attempts were made to realise an aqueous solution of selenourea but a reddish suspension developed due to reduction of selenourea to Se. The same effect was observed in ethanol solvent. Finally a colourless stable solution was obtained by dissolving selenourea in 99.98 % acetone. $InCl_3$ is insoluble in acetone therefore it was dissolved in a mixture of 85 % acetone and 15 % water and the concentration adjusted to 0.1 M. The appropriate equivalent volumes of each solution were measured out and mixed just before the spraying cycle. The solution was observed to be physically stable over the spray cycle which lasted for 20 minutes. The substrates were 3 cm x 7 cm glass placed on a heater 12 cm below the nozzle. A bimetallic thermometer that could measure the temperature to an accuracy of ± 1 K was used to measure the substrate temperature. All the parts of the equipment besides the gas supply and solution vessel were housed in an air tight shield fitted with an exhaust to reduce contamination by the atmosphere. In the absence of adquate literature it was first important to optimise the precursor solution concentration. A set of films were prepared at 523 K for different Se/In atomic ratios of 0.5, 1.5, 2.0 and 4.0 so as to optimise the Se/In ratio. In order to investigate the effects of T_{sub} on films properties, the optimum Se/In ratio and all the other parameters indicated were kept constant. A set of samples were deposited at T_{sub} of 473 K, 573 K, 673 K and 723 K.

The thickness of the films was measured using a P-15 KLA Tencor stylus surface profiler. The optical transmittance and reflectance for all wavelengths in the range of $300 < \lambda < 2500$ nm (to an accuracy of ± 0.1nm in the UV-VIS and 0.4nm in the NIR) were measured using a Cary 500 scan UV/VIS/NIR spectrophotometer. A Keithley based four point probe was used for electrical calibrations. The morphology of the films was studied by using X-ray diffraction data obtained from a Philips (PW3710) X-ray Diffraction (XRD) system. The radiation used was cu-Kα 1 with a wavelength of 1.54056Å within the values of 2θ between 5.01-74.9 degrees. The surface of the films was studied using an XL 30 ESEM scanning electron microscope. The elementary composition of the films was determined from results obtained from Energy Dispersive X-rays (EDX).

3. Results and analysis

Fig. 1and 2 shows X-ray diffraction (XRD) bitmaps of films prepared at different selenium to indium atomic ratio (Se/In) in the starting solution at a T_{sub} of 523 K and different T_{sub} with a Se/In ration of 1.5 respectively. This temperature was chosen because the ratio of Se/In in the films as determined from EDX measurements showed a small deviation (Δ_c) from that in the starting solution. The value of Δ_c was less than 2.0 % and therefore the Se/In ratios referred to herein are essentially the values in the starting solutions.

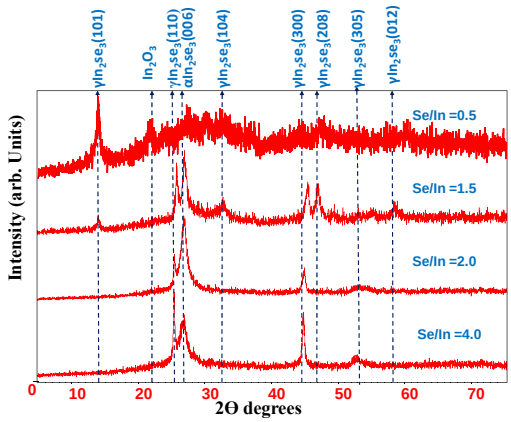

Fig. 1. XRD bitmaps of In_2Se_3 films prepared at different Se/In.

Table 1. Grain sizes (D), dislocation density (δ), EDX Se/In values, deviation of Se/In value from that of the starting solution (Δc), O_2 impurity concentration, resistivity (ρ), extinction coefficient (k) (550 nm) and figure of merit (F_M) in the films fabricated at different substrate temperatures.

T_{sub} (K)	D (nm)	δ (cm^{-2})	Se/In	Δc (%)	O_2 (at.%)	P (Ω cm)	k	F_M (Ω^{-1})
473	240	1.74×10^9	1.52	1.33	14.7	$>10^6$	0.014	$>10^{-11}$
573	290	1.19×10^9	1.46	-2.67	9.6	2.51×10^4	0.027	6.36×10^9
673	320	9.77×10^8	1.37	-8.67	4.4	5.88×10^2	0.103	7.22×10^8
723	210	2.27×10^9	1.22	-18.7	-	7.31×10^2	0.073	8.27×10^8

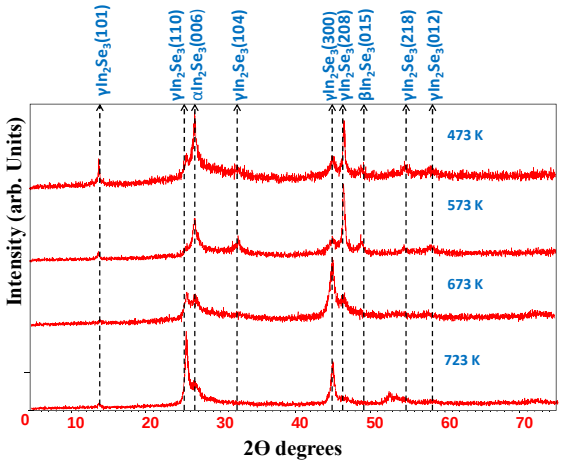

Fig. 2. XRD bitmaps of In_2Se_3 films prepared at different substrate temperatures.

Fig. 3(a-c) shows low T_{sub} mechanism of film growth starting from nucleation sites, then isolated islands and finally a continuous film. On the onset, growth is marked by isolated islands around nucleation sites. At low temperatures, it is anticipated that there is simultaneous growth around nuclei owing to low surface mobility of the adatoms. As film growth advances, the islands touch but spaces are trapped between the boundaries. This boundary defects are significant in that they act as collection centres for impurities diffusing out of the lattice hence act as scattering sources for photons and carriers. Impurities may build potential barriers with the film with consequent modifications in the film electrical properties. The film surface was rough and porous with poor stacking. At 573K (3d) and 673 K (3e), the film is smoother, less cracked and better adhered to the substrate. At 723 K (3f-h), the film was extensively cracked with cracks average 90 nm. The cracking maybe due to mismatch in linear expansivity of the brittle film and glass substrate. Such cracking has been previously reported by others for this material [22]. This mismatch was confirmed by cooling the film rapidly which left the surface extensively warped, cracked and peeled off (3h). It was observed that at higher T_{sub} (723 K) there was deviation from spherical grain growth towards a mesh like network of crosslinked fibres. Embedded in these fibrous networks, are uniformly dispersed nanospheres (not visible here) of average diameter of 52 nm. It was not clear whether these nanospheres were In_2Se_3, Se or In but looking at the excess of indium at this T_{sub}, it is a worthwhile assumption that these are indium nanospheres. These structural adjustments arising from substrate temperature effects are well evident in XRD bitmaps (Fig. 2) and are indicated by the varying crystallographic orientations and peak intensities.

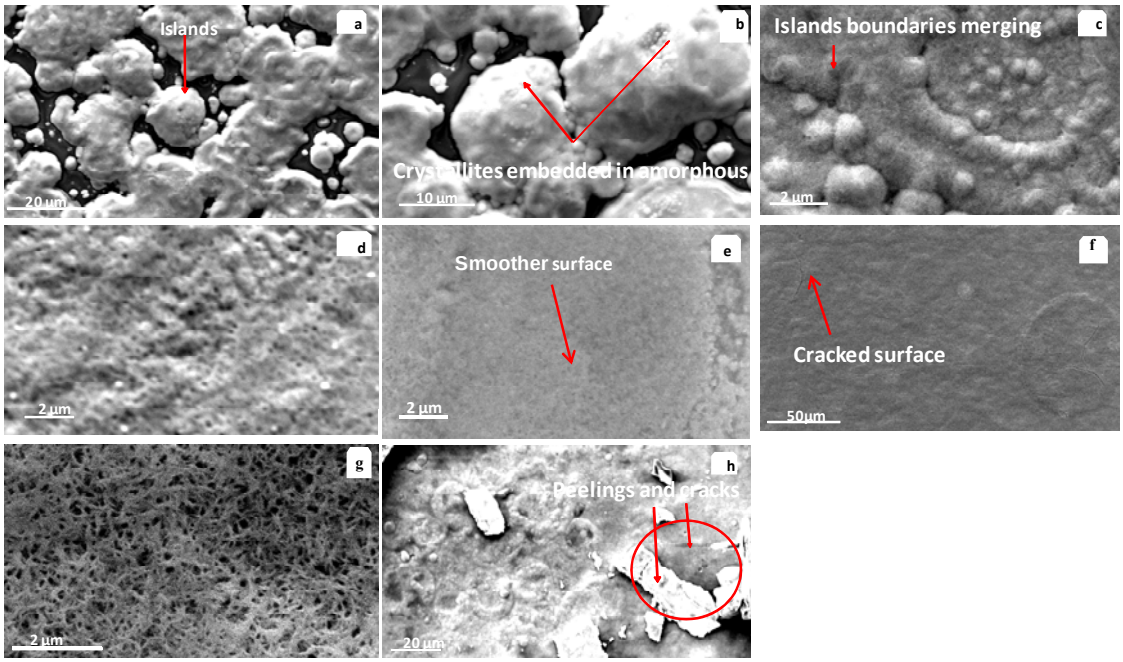

Fig. 3: SEM pictographs of In_2Se_3 thin films prepared at 473 K (a), (b) and (c), 573 K (d), 673 K (e), 723 K (f), (g) and a film prepared at 723 K followed by rapid cooling (h)

The grain sizes (Table 1) were approximated from SEM surface scans of the films by matching the linear scale provided in the pictographs and statistical sampling of the grains images and also correlated from the Deby-Scherer equation; $D = k\lambda/(\beta\cos\theta)$ [23], where k is the Scherer's constant ,λ is the wavelength of the X-ray used, β is the full width half maximum and θ is the Bragg's angle in radians. The crystallite dislocation densities (δ) were obtained from the expression; $\delta = n/D^2$ [24], where D is the grain size and n is a constant close to unity.

Values of D and δ are listed in table 1. The grain sizes increased from 240 nm at 473 K to 320 nm at 673 K and then reduced to 210 nm at 723 K. According to the 'survival of the fastest model' [25] elevated T_{sub} increases the kinetic energy and lifetime of the adatoms on the substrate surface therefore only low surface energy nucleation sites grow larger. At low T_{sub} due to low surface energy of adatoms, there are many competing phases and orientations which lead to low grain size. At higher T_{sub} the adatoms have higher mobilities over the substrate and end up resting in the nucleation sites corresponding to lowest surface energy and hence shift growth towards certain preferred orientation (γ-In_2Se_3) and larger grains. T_{sub} above optimum encourages re-evaporation of deposited material and solvent evaporation occurs above substrate which results to low grain size and high porosity. The obtained values of δ are consistent with the observed change in crystallinity and grain size.

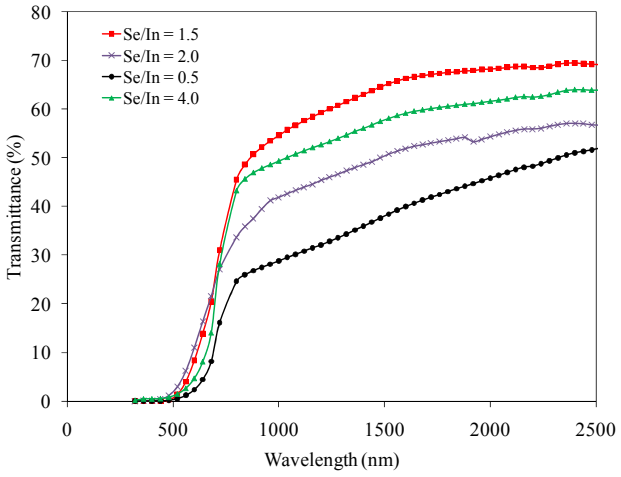

Fig. 4. Spectral dependence of radiation transmission through In_2Se_3 thin films for Se/In = 0.5, 1.5, 2.0 and 4.0 prepared at a T_{sub} of 523 K.

Fig. 4 represents the transmittance of films measured within the wavelength 300-2500 nm range for In_2Se_3 prepared at Se/In values of 0.5, 1.5, 2.0 and 4.0 in the starting precursor solutions. It can be concluded that films prepared at Se/In = 1.5, which is the stoichiometric composition, showed highest transmittance in the wavelengths measured. Increase in Se above this ratio reduced the transmittance and shifted the cut off wavelength towards longer wavelengths. On the other hand, it is observed from the transmittance curves shown in Fig. 5 that the highest transmittance was at lower T_{sub}. This we think is due to presence of impurities (mainly oxides) and changes in the crystallographic orientations of the In_2Se_3 phase induced by variation of the T_{sub}, a supposition confirmed by XRD measurements. The cut off wavelength also shifted to lower wavelength with decreasing T_{sub}.

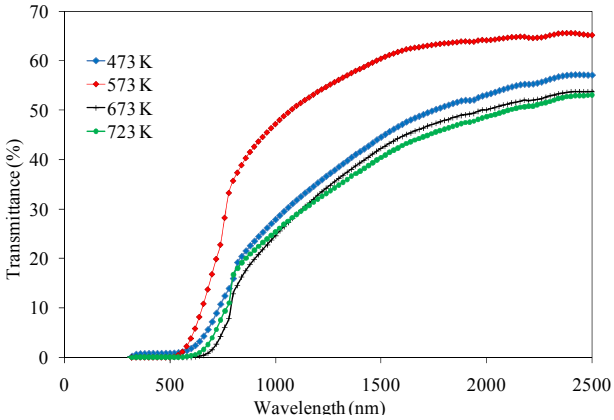

Fig. 5. Spectral dependence of transmittance for In_2Se_3 films as a function of T_{sub}.

Optical transmittance (T), reflectance (R) and film thickness (t) are related to the absorption coefficient (α) by the relation [26];

$$\alpha = (1/t)\,ln\,((1-R)^2/T) \qquad (1)$$

It is well known [27] that the absorption coefficient, α, energy gap (E_g) and photon energy (hυ) are related by the expression;

$$\alpha = A\,(h\nu - E_g)^n/h\nu \qquad (2)$$

where A is a constant that follows the slope of a plot of $(\alpha h\nu)^{1/n}$ vs $h\nu$ called the Tauc's plot [27]. The parameter n depends on the nature of transition of excited carriers and assumes a value of ½ or 2 for direct allowed and indirect allowed respectively and 2/3 or 3 for direct or indirect forbidden transitions. Indium selenide exhibits direct allowed transitions and n has a value of ½ [11]. From the Tauc's plot (Fig. 6), extrapolation of the linear part to the x-axis where α reduces to zero gives the band gap of the material. All samples show the exponential Urbach absorption edge behavior coupled with a near energy-independent absorption tail tending towards lower energies. Considering that SEM pictographs confirm polycrystalline grains embedded in an amorphous matrix, the tails in the absorption spectrum were described in terms of indirect transitions and disorder in the films [28]. The values of the absorption coefficient were in the order of 10^{-4} cm^{-1}. The optical band gap decreased from 2.60 eV at Se/In value of 0.5 to 2.21 eV at a Se/In value of 4.0. Physical examination of a film with Se/In =0.5 indicated reddish yellow colour and showed more transparency in the visible range. The observed large band gap and colouration at Se/In=0.5 are characteristic of presence of wide gap In_2O_3 impurities as confirmed by XRD studies.

The band gap was found to be T_{sub} sensitive as shown in Fig. 7. The band gap was found to decrease from 3.62 eV at 473 K to 1.92 eV at 673 K. At 473 K the plots indicates two band gap values (2.18 and 3.62 eV) corresponding to α and β phases as indicated by XRD results. Double band gap corresponding to the two phases was also observed in the same material by another study [29] at low T_{sub} (373-473 K) for annealed Se/In bilayers prepared from chemically deposited Se and evaporated indium. However our values are higher which may be due to the band gap stretch by impurities at low T_{sub}.

Generally, increase in the T_{sub} was found to decrease the value of the band gap which can be attributed to introduction of other secondary phases such as In_2O_3 at lower T_{sub}. There was a slight increase in E_g for an increase of T_{sub} from 673 K to 723 K which can be attributed to increase of disorder in the film and change from nanosperical growth to nano-fibres as confirmed by deviation from preferred orientation and film structure with this temperature adjustment. Bounzouita *et al.*, 2002 [10] observed pronounced presence of oxygen in InSe films prepared at lower substrate temperature of 523 K which reduced for a T_{sub} of 573K with a subsequent decrease in the energy gap. It is anticipated that at a T_{sub} of 473 K there was some amount of oxide in the films although this was not indicated by XRD measurements. We think that this latent oxygen may be due to the amorphous nature and the fact that In_2O_3 main peak lies in the region of amorphous glass hump, but physical examination of the films revealed reddish yellow colour which was an indication of this oxide. Films prepared at 673 K and 723 K were grey in colour and looked glasslike with reflective surfaces. The optimum band gap of 1.92 eV was obtained at 673 K and this value agrees closely with earlier reported values [14, 19, 30] for films prepared using other methods.

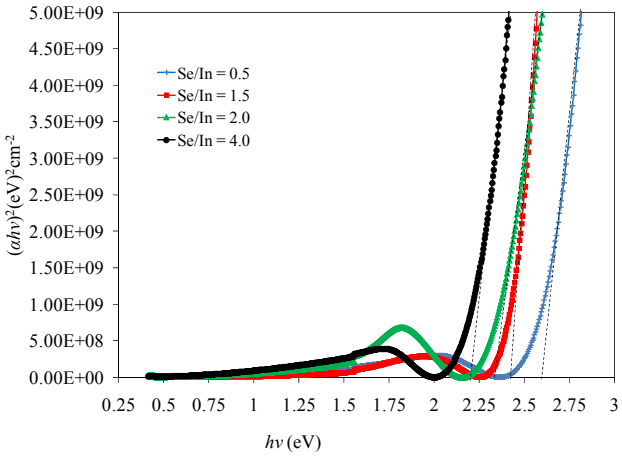

Fig. 6. Determination of E_g from the plot of $(\alpha h\nu)^2$ and energy of incident photons for In_xSe_y for films prepared at a T_{sub} of 523 K . Se/In = 0.5, 1.5, 2.0 and 4.0 .

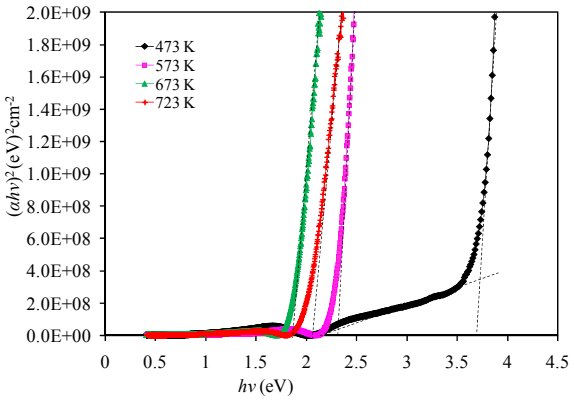

Fig. 7. Plot of $(\alpha h\nu)^2$ and energy of photon (eV) for In_2Se_3 films prepared at different T_{sub}.

An ohmic behaviour was exhibited in the dark conductivity mode at room temperature (300 K). The lowest resistivity (ρ) of 587.9 Ω cm was recorded for a sample prepared at 673 K. Hot probe studies show n-type conductivity. Films prepared at lower T_{sub} (473 K) were highly resistive in the order of 10^6 Ω cm due to boundary scattering effects, potential barriers arising from impurities and formation of α-In_2Se_3 which is known to be highly resistive. The resistivity at 723 K was higher which we think is due to shift in film growth to loosely stacked nanosized fibers and discontinuity in the film as a result of cracking and warping. The figure of merit ($F_{M=}1/\rho\alpha$) [31] was calculated and values obtained at 550 nm listed in Table 1. The figure of merit was low at lower T_{sub} and increased with T_{sub} from 6.36 x10^{-9} Ω^{-1} at 573 K to 7.22 x 10^{-8} Ω^{-1} at 673 K then increased slightly to 8.27 x10^{-8} Ω^{-1} at 723 K. The observed trend is consistent with the improved texture and crystalline nature of the samples at intermediate temperatures.

4. Conclusion

Glass like γ-In_2Se_3 thin films were successfully prepared by spray pyrolysis at higher T_{sub}. The film properties were found to be sensitive to preparative conditions and composition. Low T_{sub} favoured amorphous growth and incorporation of impurities. At higher T_{sub} there was increased grain growth, increased crystallinity and optical band gap shift towards the bulk value. However, these higher temperatures reduced film adhesion, introduced surface deformations and reduced Se/In ratio in the films. Measured parameters at optimum conditions are; direct band gap of 1.92 eV grain size 320 nm and n-type conductivity with dark resistivity of 587.9 Ω cm obtained at 300 K. Films prepared at a T_{sub} of 673 K and Se/in ratio of 2.0 were found to be superior in terms of targeted properties for application as an energy window in chalcopyrite solar cells.

Acknowledgements

The authors would like to thank African Materials Science and Engineering Network (AMSEN), a Carnegie IAS-RISE network for financial assistance and the University of Botswana for providing research facilities.

References

[1] A. Madan, M.P. Shaw, The Physics and Applications of Amorphous Semiconductors, Academic press, Boston (1988)
[2] N. Mehta, J. Sci. Ind. Res. **65**, 777 (2006)
[3] M.A. Popescu, Non-crystalline Chalcogenides, Kluwer Academic Pubishers, Dordrecht (2000)
[4] N. Mehta, A. Kumar, Journal of Therm Anal. Calorim. **87**, 343 (2007)
[5] G. Gordillo, C. Calderón, Sol. Energy Mater. Sol. Cells **77**, 163 (2003)
[6] J. V. McCanny, R B Murray, J. Phys. C: Solid State Phys. **10**, 1211 (1977)
[7] H. Lee, Dae-Hwan Kang, L. Tran, Mater. Sci. Eng. B **119**, 196 (2005)
[8] R. Vaidyanathan, J.L. Stickney, S. M. Cox, S. P. Compton, U. Happek, J. Electro. Chem. **559**, 55 (2003)
[9] M. Yudasaka, T. Matsuoka, K. Nakanishi, Thin Solid Films **146**, 65 (1987)
[10] H. Bouzouita, N. Bouguila, S. Duchemin, S. Fiechter, A Dhoui, Renewable Energy **25**, 131 (2002) .
[11] K.M. Beck, W. R. Wiley, E. Venkatasubramanian, F. Ohuchi, Appl. Surf. Sci. **255**, 9707 (2009).
[12] H.M. Pathan, S.S. Kulkarni, R.S. Mane, C.D. Lokhande, Mater. Chem. Phys. **93**, 16 (2005).
[13] S. Shigetomi, H. Ohkubo, Ikari, Thin Solid Films **199**, 215 (1991).
[14] D.Y. Lyu, T.Y. Lin, J.H. Lin, S.C. Tseng, J.S. Hwang, H.P. Chiang, C.C. Chiang, S.M. Lan, Sol. Energy Mater. Sol. Cells **91**, 888 (2007)
[15] S. M. El-Sayed, Vacuum **72**, 169 (2004)
[16] J. Hupkes, B. Rech, O. Kluth, T. Repmann, B. Zwaygardt, J. Muller, R. Drese, M. wuttig, Sol. Energy Mater. Sol. Cells **90**, 3054 (2006)
[17] M. Krunks, O. Bijakina, T. Varema, V. Mikli, E. Mellikov, Thin solid films **338**, 125 (1999)
[18] M. R Asabe, P. A Chate, S. D Delekar, K. M Garadkar, I. S Mulla, P. P Hankare, J. Phys. Chem. Solids **69**, 249 (2008)
[19] K. Bindu, C. S. Kartha, K.P. Vijayakumar, T. Abe, Y. Kashiwaba, Appl. Surf. Sci. **191**, 138 (2002)
[20] J. Clavijo, E. Romero, G. Gordillo, J. Phys. Conference Series **167**, 012016 (2009)
[21] C.M. Muiva, T.S. Sathiaraj, K. Maabong, Ceramic International **37**, 555 (2011)
[22] Aytunc- Ates, M. Kundakc, A. Astam, M.Yildirim, Physica E **40**, 2709 (2008)
[23] B.D. Cullity, S.R. Stock, Elements of X-Ray Diffraction, Prentice-Hall, New York (2001)
[24] G.K. Williamson, R.E. Smallman, Philosophical Magazine **1**, 34 (1956)
[25] Van der Drift, Philips Res. Rep. **22**, 267 (1967)
[26] J. Pankove, Optical Processes in Semiconductors, Prentice-Hall Inc., New Jersey (1971)
[27] J. Tauc, R. Grigovici, Y. Yanca, Phys. Stat. solidi **15**, 627 (1966)
[28] C. Baban, G.I. Rusu, Appl. Surf. Sci. **211**, 6 (2003)
[29] R. Sreekumar, R. Jayakrishnan, C. Sudha Kartha, K.P. Vijayakumar, Y. Kashibawab, T. Abe, Sol. Energy Mater. Sol. Cells **90**, 2908 (2006)
[30] K.J. Changa, S.M. Lahnb, Z.J. Xiec, J.Y. Changa, W.Y. Uenc, T.U. Lud, J.H. Lind, T.Y. Lin, J. Cryst. Growth **306**, 283 (2007)
[31] R.G. Gordon: Mater Res. Soc. Symp. **426**, 419 (1996)

*Corresponding author: cmuiva@yahoo.co.uk